Sudden degradation of asphalt road mixes during periods of freeze-thaw events: Analysis of field cases and exploratory laboratory research

Valéry MAUDUIT
Direction Interdépartementale des Routes du Massif Central, Issoire, France

Caroline MAUDUIT
CETE de Lyon, LRPC de Clermont-Ferrand, France

Nelly VULCANO-GREULLET
DREAL Bourgogne, Dijon, France

Nathalie COULON
CETE de Lyon, LRPC Autun, France

Ferhat HAMMOUM, Hamon DAVID, Jean Pierre KERZREHO, Jean Michel PIAU, Armelle CHABOT
Université de Nantes-Angers-Le Mans, IFSTTAR, Bouguenais, France

ABSTRACT

In light of the damage witnessed on France's road network over the past winters, network managers and the scientific community have been seeking to understand the phenomena at play in order to prevent against such degradation. The research undertaken between 2006 and 2009 by the "water-freezing" working group as part of LCPC's Fondephy research project[1] has allowed for an in-depth investigation of a few field cases and the generation of leads for future studies regarding the damage mechanisms capable of taking place over both the long and short term. Among these mechanisms, the phenomenon of sliding, recently observed on the Nantes pavement fatigue carrousel, has been noted between wearing course and foundation layer; this finding has altered the generally held perception of pavement operations specific to the overlaying of bituminous layers and may justify a fatigue occurring over the upper part of the pavement, exacerbated at higher temperature. From another perspective, the phenomenon of swelling of frozen asphalt mixes exposed to partial water saturation could also be explored thanks to recent observations during laboratory experiments that had been inspired from soil freezing/thawing test campaigns. This mechanism may give rise to the sudden appearance of potholes at the pavement surface when exposed to winter weather conditions.

Dégradation subite des enrobés bitumineux par période de gel/dégel : analyse de cas de terrain et recherche exploratoire en laboratoire

RÉSUMÉ

Suite aux dégâts rencontrés sur le réseau routier français ces derniers hivers, les gestionnaires de réseau et la communauté scientifique ont cherché à comprendre les phénomènes mis en jeu afin de prévenir de telles dégradations. Les travaux menés entre 2006 et 2009 par le groupe de travail « eau-gel » de l'opération de recherche Fondephy[1] du LCPC ont permis d'investiguer en détail quelques cas de terrain et d'apporter des pistes de réponse, quant aux mécanismes d'endommagement à long et court terme susceptibles de s'être mis en place. Parmi ceux-ci est évoqué un phénomène de glissement, récemment observé sur le manège routier de Nantes, entre couche de roulement et couche de base, qui modifie la perception du fonctionnement généralement admis, de la superposition de couches bitumeuses et qui pourrait justifier d'une fatigue en partie haute de chaussée, notamment à température élevée. Dans un autre ordre d'idée, on rend compte du phénomène de gonflement au gel d'enrobés bitumineux partiellement saturés en eau, récemment observé également, au cours d'expérimentations en laboratoire, inspirées des essais de gel/dégel sur sols. Ce mécanisme pourrait être à l'origine de l'apparition subite de nids de poule en surface de chaussée, en conditions hivernales.

[1] *http ://or.lcpc.fr/fondephy*

BACKGROUND

During the 1970's and 1980's, France's primary road network was significantly reinforced and today is mainly composed of thick, semi-rigid or composite asphalt structures (Setra-LCPC, 1997). Since their construction, wearing courses have been renewed several times through either replacement or covering. Over the past few years however, deterioration has appeared at the end of the winter season on wearing courses of certain heavily-trafficked roads. These degradations take the form of series of potholes, sometimes occurring on long distances (several tens of kilometres); such structural disorders are also noteworthy for their capability of appearing very quickly without any specific preliminary indication or precursor (Mauduit *et al.*, 2007). Their consequences are disastrous for road users, especially when the magnitude of degradations leads road managers to shut down the affected traffic lanes.

Road network managers have requested that the scientific community analyse this phenomenon, for the purpose of: improving its understanding; refining pavement behaviour modelling tools; predicting the risk such degradations appear on the existing network; and proposing measures to prevent the phenomenon from recurring.

This article presents the research conducted between 2006 and 2009 by the "water-freezing" working group assembled during the LCPC project entitled *Fondephy*, which stands for "physical bases for the mechanical behaviour of materials in pavement structures", in an attempt to determine the set of factors and causes of the observed disorders. Two actions were executed in parallel. The first, set forth in Section 2 below, entailed collecting and analysing several field cases typical of this type of degradation with adequate documentation (Vulcano *et al.*, 2010). A correlation was also drawn with relatively recent and new observations, recorded during experiments on the LCPC/IFSTTAR pavement fatigue carrousel relative to high-temperature operations occurring at pavement layer interfaces. The other action pertained to the laboratory study of freeze-thaw behaviour of partially water-saturated asphalt concretes (AC), by means of transposition to these materials from tests typically carried out *in situ* on soils (Mauduit *et al.*, 2010).

FEEDBACK FROM THE FIELD

Many degradations have appeared on road networks both in France and abroad over roughly the past decade. A few cases have been specifically documented in the United States (Kandhal *et al.*, 2001), Canada and Australia (Fromm *et al.*, 1969; Kandhal *et al.*, 1989; Hicks, 1991; Kandhal and Rickards, 2001). Work completed as part of the *Fondephy* project has focused on the few field cases recently observed in France, as characterized by a sudden and extensive appearance of potholes during winter (Vulcano-Greulet *et al.*, 2010). These cases have led to assembling (by re-establishing contact as needed with road contractors or re-evaluating independent inspection reports on road works) a rather broad spectrum of information on: the pavement structure, the maintenance program, traffic levels, date of construction, periodicity of phenomenon appearance, location across the French territory, climate stress, etc. Two cases will be reported herein for purposes of illustration.

Pavement located in north-eastern France (sudden disorders observed in 2005)

This studied pavement was carrying a daily traffic load of 2,700 trucks. The layout, featuring a 5% slope, crosses hilly zones subjected to a continental climate characterized by relatively hot summers and cold, wet winters. Over the examined section, the pavement structure is of the semi-rigid type (Setra-LCPC, 1997). The base layers are composed of 50 cm of a 0/20 silico-calcareous, gravel-slag mixture set into place in the 1970's. Since the time of construction, three maintenance campaigns had involved reloading materials, which led in 2001 to a pavement structure containing up to 35 cm of hydrocarbon materials.

A visual recording of degradation undertaken in 2001 displayed, on the 2-km section under study, crazing-type degradations along the slow-traffic lane. Subsequent to stripping that occurred during heavy summer rains, a 1-km maintenance operation was performed on the down-slope part. This maintenance program consisted of restoring the surface layer after planning the wearing course and just a portion of the binder course. The materials introduced in these AC have been local (of the alluvial type) containing sand-lime, andesitic basalt or micro-diorite. For these materials, adhesion characteristics with respect to the binder may in some instances be defective and often require adding an interface adhesion agent. The binder used as a surface layer (binder course plus wearing course) is a 35/50 multi-grade type specially adapted for zones with high rutting risk (on-/off-ramps, slow lanes, etc.).

The visual recording of degradation performed in 2005 shows, over the first kilometre of section not reassessed in 2001, distinct transverse cracks covering 10% of the surface and distinct longitudinal cracks on the traffic lane over 30% of the surface. No indication of any other degradation or stripping was noted.

During the winter season 2005/2006, within just a few days, many potholes appeared over the first kilometre of the section (see **Fig. 1**), requiring emergency repairs, several times a day in some places. These potholes, of a size in the tens of square cm and 5 to 12 cm deep, are plentiful, tightly spaced from one to the next and located in their entirety on the slow-traffic lane, predominantly in the wheel tracks. The borehole samples extracted on this portion of pavement, following these events, reveal that the foundation treated with a hydraulic binder remains in very good condition, with a thin AC bonded to it. The cracked and crazed wearing course lies on two non-cohesive layers, with the presence of hydrocarbon materials that display considerable stripping.

Figure 1
Pavement disorders in north-eastern France
(a) Pavement structure borehole sample
(b) Pattern of potholes tens of cm in size

Pavement located in central France (disorders found in 2010)

This study pavement stems from a motorway onramp, whose 1-km alignment follows a slight curve with a single incline of 1% in direction 1 heading towards direction 2. In 2009, truck traffic was limited to 860 a day for a total average traffic of 20,000 vehicles/day. This suburban pavement crosses a plain with a dry subcontinental climate featuring significant thermal and moisture variations. This inverse compound structure was built in 1996 with the following bottom-to-top composition: 25 cm of sand-cement mix (SC), 12 cm of unbound granular material (UGM), 8 cm of dense asphalt material for base course (DA), 6 cm of medium coarse asphalt (MCA) and 4 cm of porous asphalt (PA). At present, after patching in year 2000 of the PA by a discontinuous thin asphalt concrete (TACa), the WRC was raised, in both traffic directions, by 22 cm of hydrocarbon binder-treated materials. The tack coats were present and well proportioned. Pavement materials are of the basalt and rhyolite type, without the addition of adhesive agents. The hydrocarbon binder introduced on both the MCA and PA is a multigrade bitumen, while the binder of the thin asphalt concrete (TAC) cover layer is a pure 50/70-grade bitumen. In 2008, a field inspection exposed longitudinal cracks on the wearing course in direction 2 that had not been cited in the IQRN (national road network

index quality) score, due to the adopted quality assessment method that had solely addressed direction 1 on a bidirectional pavement.

At the end of January 2010, potholes were forming within a very short interval, making it necessary to close the section. The dimensions of these potholes were larger than 10 square cm and their depth in some instances reached 15 cm. These flaws were observed on the wearing course in direction 2, on a length extending more than 500 m, which for the most part corresponds to the low point of the road profile. It could also be observed that the pavement structure was loaded, despite being built as an embankment, since the potholes were filling within a few minutes when empty **(Fig. 2a)**. The onsite borehole coring campaign displayed disaggregation of the asphalt concrete at the level of the first interface **(Fig. 4b)**, in this case at a depth of several cm.

Figure 3 reports on winter weather conditions experienced onsite during the month of January 2010. Let's note the presence of many daily freeze-thaw cycles ($T_{min} < 0$, $T_{max} > 0$ on the same day) with strong daily temperature amplitudes (-4° to +7°C within an 8-hour period) and precipitation in liquid form.

Figure 2
Observations recorded on test section 2 (central France specimen) (a) Rise of a head of water in a pothole in the PA layer (b) Borehole sample with disaggregated PA

a b

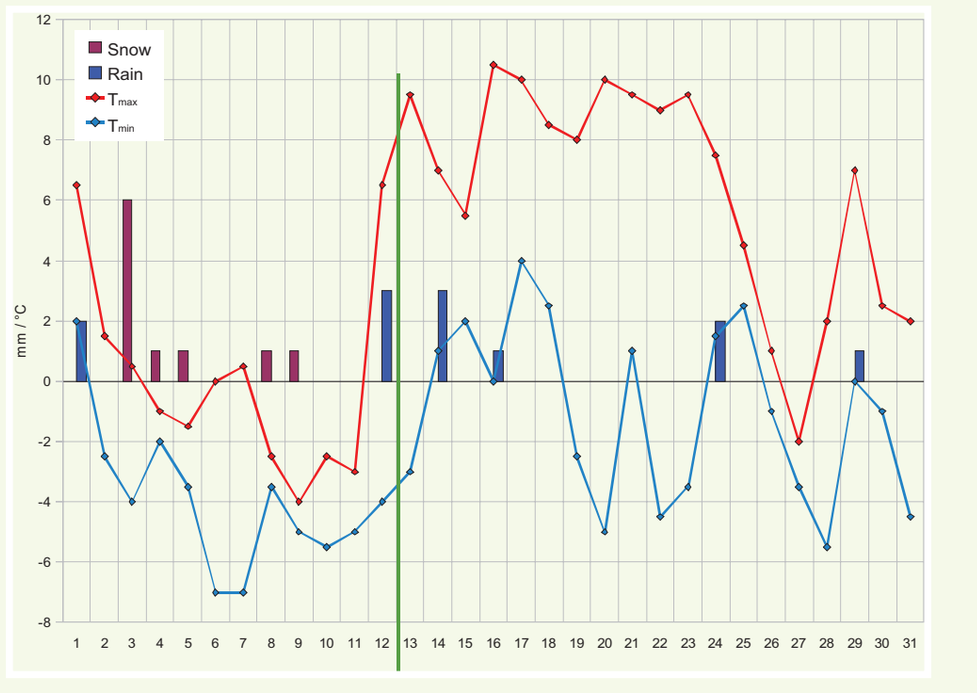

Figure 3
Meteorological recording from January 2010, provided by the Météo France weather station (located less than 3 km from the degradation zone)

Analysis of probable degradation causes

The circumstances surrounding the appearance of disorders like those described above serve to verify the existence beyond any doubt of a specific mechanism that leads to a widespread formation of potholes over a very short time interval. This recognition raises the following questions: what exactly are the underlying mechanism and its associated factors? Is this mechanism by itself sufficient to explain the entire set of phenomena or is its influence on pavement reaction more "modest", given the fact that the pavement condition would have already been degraded by more long-term damage mechanisms?

In response to these questions, three factors were emphasized, namely: the role of traffic, the presence of water in the pavement, and temperature variations.

› The impact of traffic

Traffic, as expressed in millions of expected truck trips over the pavement life cycle, is normally considered as the predominant factor of long-term pavement degradation due to fatigue. According to the French pavement design method, this factor is in large part responsible for determining the size of all structural layers.

In the cases studied herein, this factor most certainly plays a role during the rapid evolution phase, as evidenced by pothole locations, which are basically laid out along the wheel tracks. Yet at this time scale, such an influence can only be secondary and not a fatigue effect, according to the standard meaning of the term, given that the number of trucks passing during the few peak hours of the phenomenon is no more than in the range of 1,000.

On the other hand, it is entirely possible that traffic level has been able to contribute to long-term fatigue over the upper part of the pavement, leaving this part even more vulnerable to freeze-thaw cycles. A potential mechanism of this type however is to be sought beyond the typically adopted operating pattern for asphalt pavements, which assumes a compressive behaviour and hence no fatigue of layers located at the top of the pavement. Moreover, this pattern neglects the repeated shearing taking place at interfaces. Section 2.4 will show in detail why these hypotheses must be applied prudently.

› The role of water

The cases studied herein indicate the systematic presence of water in degraded pavement sections, and this occurs prior to the actual appearance of disorders. It can thus be assumed that water, in either its liquid or ice state, has played a pivotal role over the long and/or short term for the specific pathology examined. Let's recall that water accumulation in an asphalt pavement can arise in different ways **(Fig. 4)**. The most common cause is via precipitation then infiltration, to a varying extent, through the pavement surface coating, whether intact or already degraded. Water infiltration

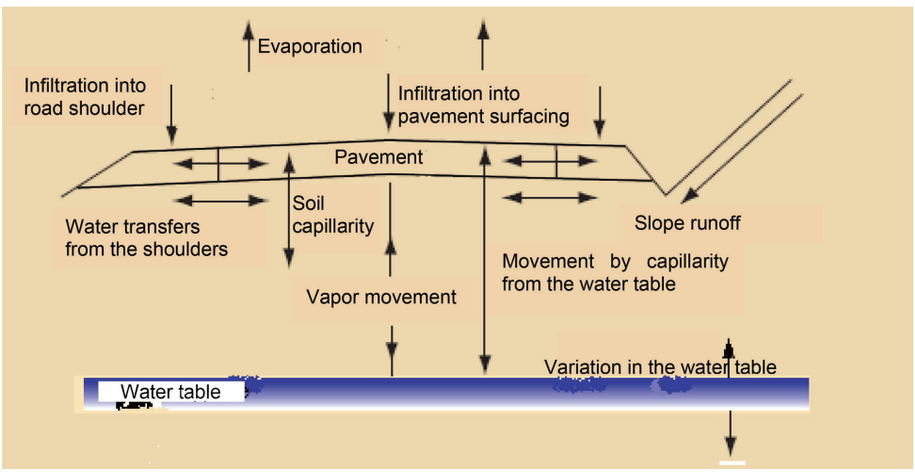

Figure 4
Water circulation both in the road foundation and pavement (Castaneda Pinzon, 2004)

can also be observed at the edges of the structure (water running off from hillsides, ditches, etc.) or else by capillary absorption from the water table or groundwater rising to the surface.

Among the factors capable of causing the arrival and/or stagnation of runoff water in the pavement are: a defective, poorly positioned or missing water evacuation system; an inadequately studied or noncompliant geometry - particularly during maintenance work - at the scale of the pavement or the superimposed layer; a suboptimal road alignment; the presence of a water source; and the expanded number of interfaces from one maintenance operation to the next. Entire zones may become saturated with water either temporarily or permanently, leading to material stripping at some point over a long-term horizon **(Fig. 5)**. It will also be seen in Section 3 however that such damaging physicochemical actions may be combined during winter with sudden mechanical effects, as potential sources of disorders, at the time of a liquid-to-ice phase change of the water contained in the pore space of asphalt concretes.

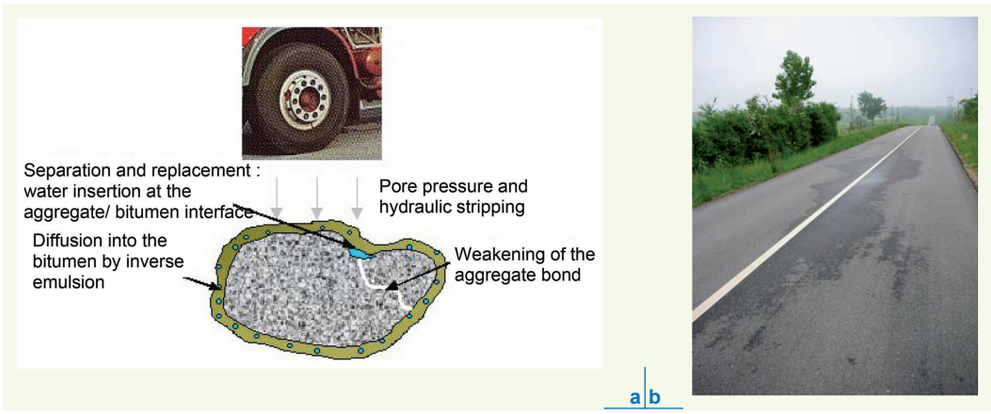

Figure 5
Effects of water (figure extracted from Castaneda Pinzon, 2004)
(a) Effects of water on the aggregate-bitumen pair
(b) Water resurgence at the pavement joint

The role of temperature

Under the hypothesis of a long-term mechanism, as a precursor to the sudden mechanism observed during winter, it was deemed pertinent to examine the effects of high temperature, which also prove to be a potential source of damage inside pavements.

› Summer temperatures

During the summer period, the effect of sunshine and temperature is well known for its capacity to generate creep and rutting of asphalt layers at the top of the pavement under the effect of traffic, depending on the granular skeleton and bitumen grades present. This mechanism however has not been identified in the cases discussed herein and, in any event, does not seem capable of causing fatigue on the top pavement layers.

It is also acknowledged that sunshine and ultraviolet rays accelerate the aging of pavement surface materials by means of bitumen oxidation, through both hardening and weakening processes. Moreover, this aging can bring about the presence, on those sections where the adopted maintenance strategy has involved material reloading, of former weakened wearing courses beneath the newly added layers. How has this type of "complex" structure evolved when subjected to the action of traffic and repeated shear loads?

Recent measurements recorded on the Nantes pavement fatigue carrousel **(Fig. 6)** have prompted a reconsideration of the actual purpose of asphalt layers at the top of a pavement.

Gauges placed on both sides of the interface between wearing course and asphalt base layer have made it possible to record the longitudinal and transverse strains created by passing "triple-axle" loads, with the middle of the tire track located in alignment with the sensors. These measurements

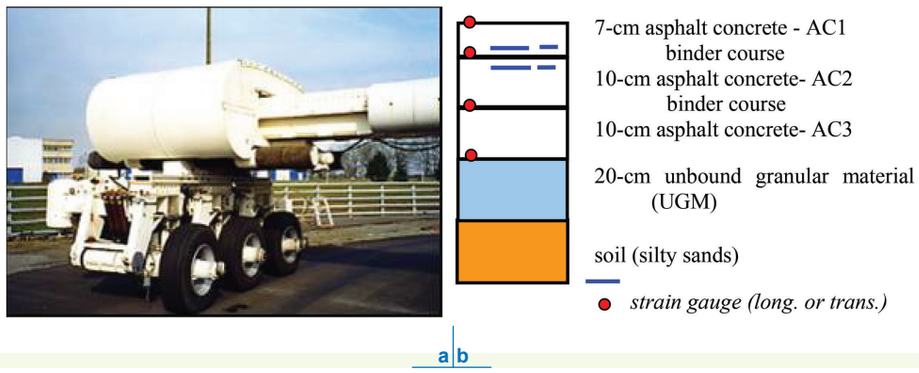

Figure 6
Measurements conducted on the LCPC (IFSTTAR) pavement fatigue carrousel (a) Wheel carriage: 3-axle, large-wheel test vehicle (b) Description of pavement structure on the instrumented carrousel

were performed for two highly-differentiated, vertical temperature profiles in the pavement, one cold the other hot **(Table 1)**.

The graphs in **Figures 7** and **8** display the responses obtained in both cases, i.e. at the bottom of the wearing course and on top of the transition layer (AC2).

A comparison of these signals in terms of both sign and intensity clearly indicates that the typically accepted hypothesis of strain continuity on both sides of the interface (i.e. the hypothesis of a

	State 1	State 2
Level	**Feb. 27th, 2009 (10:10)**	**June 4th, 2009 (15:30)**
0 cm	10°C	43°C
-7 cm	9°C	41°C
- 17 cm	9°C	34°C
- 27 cm	9°C	29°C

Table 1
Two distinct temperature states within the structure

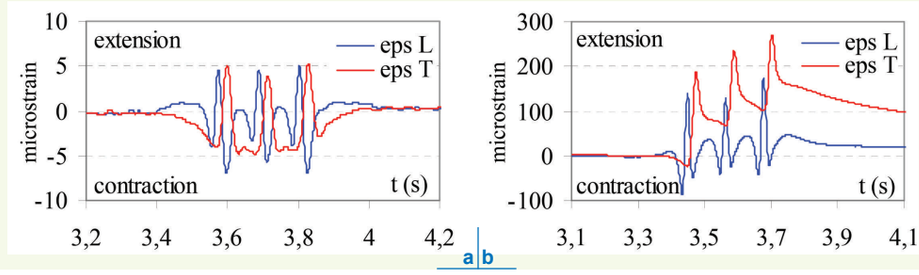

Figure 7
Strain signal at the bottom of the wearing course (a) Strains in State 1 (cold) (b) Strains in State 2 (hot)

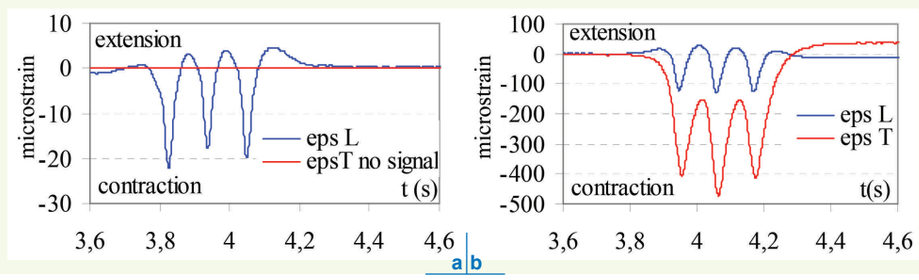

Figure 8
Strain signal at the top of AC2 (a) Strain in State 1 (b) Strain in State 2

bonded interface) has been refuted, especially at high temperature. Despite the presence of an effective and well-proportioned binder course, the 12.75-kN three-axle vehicle caused a sliding of pavement layers one on top of the other, with extensions appearing at the bottom of the wearing course that were capable of generating strong intensity, notably in the transverse direction. The degree of generality of these observations still needs to be evaluated, as do their eventual impacts on the integrity of layers and interfaces located towards the upper part of the pavement. It is not to be excluded however that this mode of operations may lead to fatigue over the upper part of the pavement (vertical and longitudinal cracking in mode I of the layers, debonding in mode II of the interfaces, etc.) and may form the basis of disorders observed during freeze-thaw episodes.

› Winter temperatures

It is obvious that the types of disorders examined herein were triggered by specific chain reactions, over an interval of a few days or even a few hours, under winter conditions. These disorders could not be completely identified down to their exact details at the given point in time, yet took place (as shown on meteorological readings) as part of freeze-thaw episodes with fast temperature variations. Moreover, it is highly likely that these conditions exerted a unique impact due to the presence of water in the AC and, as such, the rainfall (and/or snow) precipitations that fell during these episodes might have also played a role.

For this reason, an exploratory research effort was conducted in the laboratory on the freeze-thaw behaviour of AC partially saturated with water (see Section 3).

Just as summer temperatures can generate a long-term effect in weakening pavement structures prior to their sudden degradation, it is quite possible that the successive winters experienced by pavements also contribute to gradual damage, potentially originating in the same mechanism as that causing the potholes, yet with a less pronounced impact.

Along these lines, it is worthwhile to recall the results of the statistical analysis conducted on temperatures measured at the RN57 experimental site in the Vosges during the winters of 2004-2005 and 2005-2006 (Mauduit and Mauduit, 2006). These results indicate **(Table 2)** for winter 2004-2005 a large number of positive/negative (i.e. above/below freezing) temperature alternations inside the pavement: this number decreases with depth further from the pavement coating surface, spanning a range from 51 to 80.

Table 2
Number of freeze-thaw cycles at various levels in the structure at the RN 57 experimental site (Mauduit and Mauduit, 2006)

Position	Number of changes below 0°C, then above 0°C
T_a	80
T_s	80
T-2.5	74
T-5.5	60
T-8.5	51

When considering that the life cycle of a coating lasts from 12 to 15 years, it can be concluded that a coating is capable of experiencing between 500 and 1,200 freeze-thaw cycles at its surface.

It is also useful to recall that road works performed in the aim of ensuring practicability in winter are capable of causing extra “stress” on the wearing courses. Road-related weather conditions, such as snow or ice, lead road crews to undertake remedial treatments in coping with the residual film of snow (5 to 15 mm after scraping) or the ice film that formed at the coating surface. This type of action, as opposed to actions consisting of pre-emptively treating (by means of anti-icing agents) an ice accumulation risk due to the freezing of pre-existing humidity, mobilizes the latent heat of snow or ice melt in producing a relatively abrupt “thermal shock” at the pavement coating surface. **Figure 9**, derived from data measured on test sections (Boutonnet and Livet, 1990),

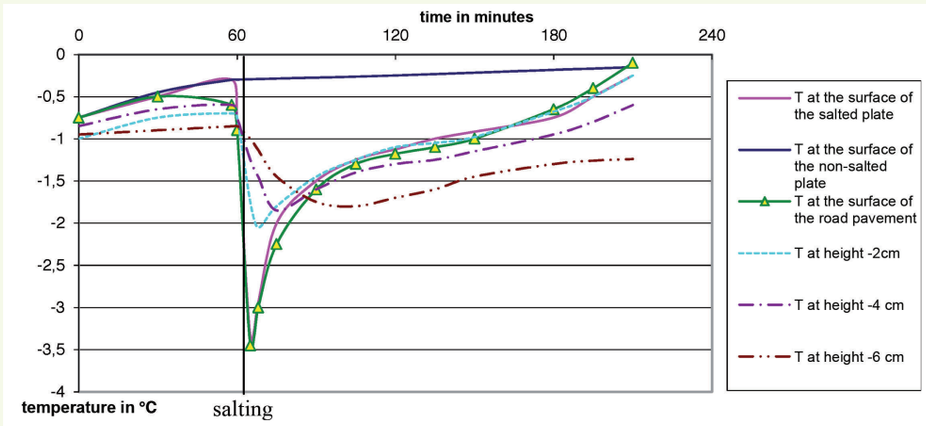

Figure 9
Thermal shock due to salting a layer of pre-existing ice on the pavement (Boutonnet and Livet, 1990)

illustrates that subsequent to a salting of 40 g/m^2 on a 2-mm thickness of ice, the coating surface temperature drops by 2.9°C. A record is also kept of the impact on temperatures measured at heights of -2, -4 and -6 cm.

LABORATORY CHARACTERIZATION OF THE EFFECTS INDUCED IN ASPHALT CONCRETES BY FREEZE-THAW CYCLES

The field observations reported above help determine the set of factors exerting a long or short-term influence on the sudden disorders appearing during winter. Yet their analysis does not indicate the specific mechanisms causing sudden material loss. In an attempt to accurately describe this loss, an original testing campaign on ACs, inspired from swelling tests during soil sample freezing, was undertaken within the scope of the Fondephy project.

The freeze-thaw behaviour of soils in the presence of capillary water has been examined for a long time, particularly in the field of road construction, and such behaviour has now been relatively well understood and effectively incorporated into analysis protocols. Three main effects are capable of arising in a soil: i) swelling during the freezing phase due to the transformation into ice of liquid water initially contained in the pores; ii) eventual exacerbation of the phenomenon by means of a cryo-suction effect increasing soil water saturation in the presence of a liquid water source (e.g. water table) located a short distance from the freezing front; and iii) the abrupt loss of mechanical properties, notably load-bearing capacity during the thawing phase.

Given the presence of such effects, experimental tests and protocols in the laboratory have been under development for many years in the aim of classifying soils with respect to their freezing/thawing sensitivity. The Ministry's RST technical network has perfected a test that allows reproducing the rise and fall of a freezing front in wet soil specimens.

As part of the Fondephy project, we sought to apply this test to the case of ACs partially saturated in water by focusing initial tests on assessing whether these ACs were also capable of undergoing swelling deformations "opposite" the expected deformations in a dry AC exposed to cooling.

The contents of this part have mainly been drawn from an article by Mauduit *et al.* (2010).

Materials employed and preparation protocol

› Choice of mix design

A 0/10 mm AC mix design resembling a classical wearing course in north-eastern France was selected for this experimental campaign. The material was produced in the laboratory from an andesitic aggregate (Trapp quarry), whose particle size distribution is presented in **Table 3** below.

Table 3
Particle size distribution of the aggregates used to produce the tested AC

Sieve size (mm)	0.063	0.5	1	2	4	6.3	10
Percent passing	7.5	15	20	29	42	58	93

A total of 48 identical samples were produced using the Duriez press: compression moulding with double effect, in accordance with the NF P 98-251-7 Standard. This production mode was selected in order to adapt the swelling installation cell size to the soil freezing steps described below (80 mm in diameter by 90 mm high). A low level of compaction was deliberately chosen for this study, so as to obtain high porosity and water content and thereby exaggerate the phenomena under observation. The average void percentages measured with a gamma densitometer lie between 8.9% and 9.4%, with a dry mix density equal to 2,602 kg/m^3.

Pore distributions were measured by means of image processing (Hammoum and Hornych, 2004) in the aim of enhancing knowledge of the pore size distribution and gaining a better understanding of measurement results. This step (not been presented herein) has shown that on one of the 48 samples, over 90% of the pore volume is composed of pores whose radii lie between 0.7 and 3.2 mm, with an average radius of less than 1.1 mm.

› Specimen saturation

A saturation procedure was adopted to speed the introduction of water inside communicating pores prior to conducting freeze-thaw testing. As a first step, samples were saturated by a pressure drop underwater. Two pressure loss levels (47 kPa and 86 kPa) were set in order to observe the influence of these pressure drops on specimen saturation. The weight of water absorbed by the sample was then used to calculate the degree of saturation S_r of each sample (Delorme *et al.*, 2007). The samples chosen for freeze-thaw testing are described in **Table 4**.

Table 4
The three samples used for freeze-thaw tests

Sample	Mass (g)	Height (mm)	Apparent density (kg/m^3)	Average void content θ_{void} measured with the gamma densitometer (%)	Pressure loss (kPa)	Degree of saturation S_r (%)
AC-36	999.2	85.81	2.317	9.2	-	0
AC-34	1001.7	86.73	2.298	9.2	47	29
AC-33	1001.1	86.26	2.309	9.1	86	51

■ Test set-up and instrumentation

› Test set-up

The testing installation allows for a “one-dimensional” freezing of cylindrical samples of the material(s) to be tested; it comprises six cells that enable simultaneously testing up to six different samples, with all cells remaining immersed in a tank containing a liquid refrigerated at a slightly positive temperature (between 1° and 2°C). **Figure 10** shows the cross-section of a cell used as part of this set-up. Freeze-thaw cycles are applied at the specimen surface via contact with a refrigerated metal piston, controlled by a cryostat. It is possible to immerse the specimen base in a subsurface flow at 1° or 2°C in order to provide a water source during the freezing phases and thus promote the cryogenic and capillary suction that may potentially ensue. The tests presented in this article were all conducted without any subsurface flow.

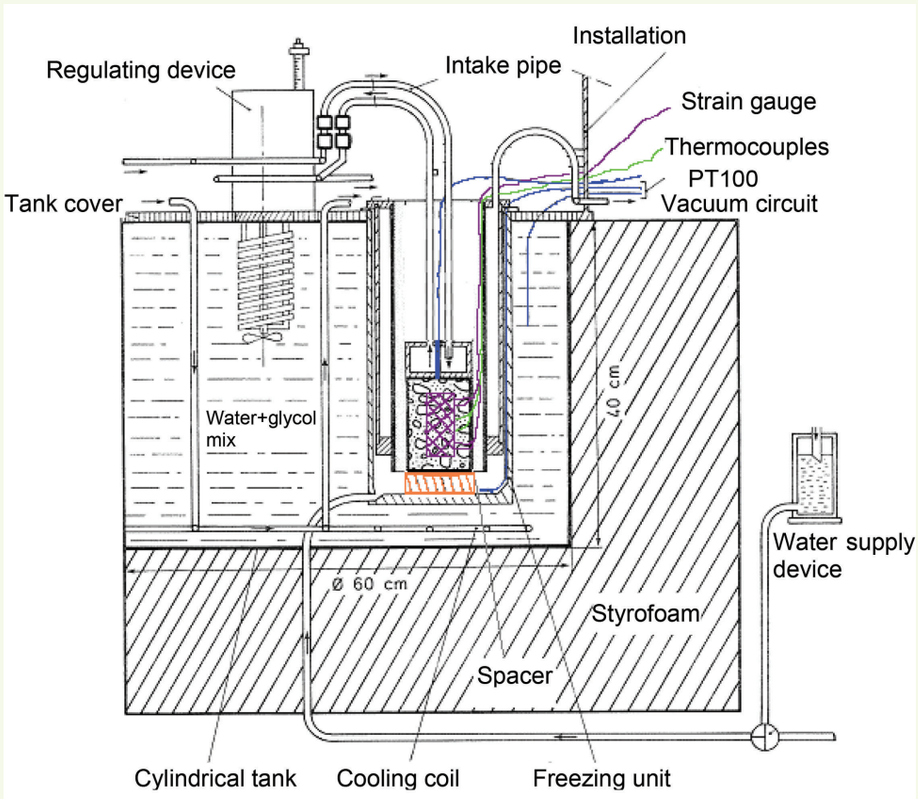

Figure 10
Cross-section of the test set-up for examining freezing/thawing on ACs

› Instrumentation

• Temperature measurements:

Preliminary tests were conducted for the purpose of determining the temperatures obtained at the sample core when freeze-thaw cycles are applied at the surface. The objective herein consisted of defining a sufficient cold intensity and cycle duration that allow reaching negative temperatures at the core and hence avoid supercooling phenomena. **Figure 11** highlights the temperature variations

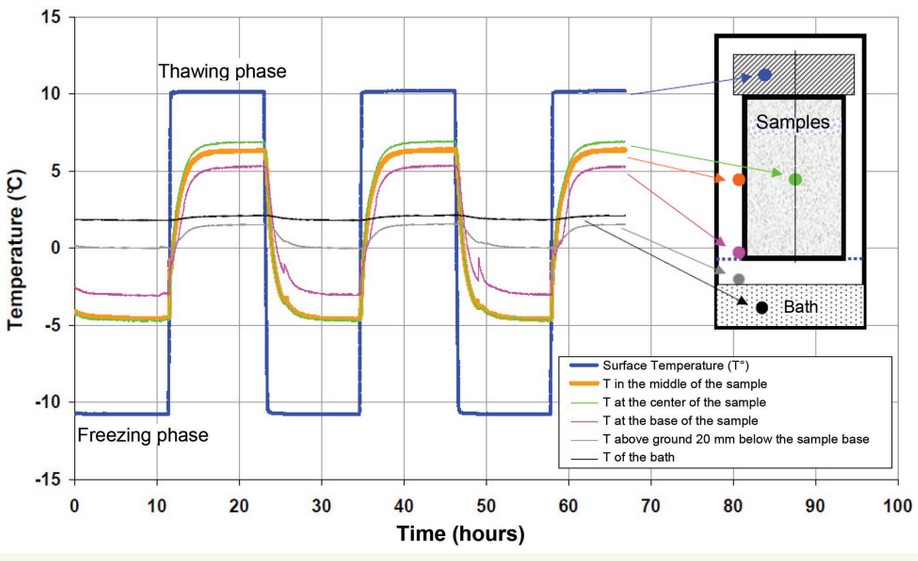

Figure 11
Temperature acquisition at various specimen levels during the freeze-thaw test

at different specimen levels during the 24-hour application period of a +10°/-10°C cycle at the surface. The extreme temperatures identified are as follows: +6.5°/-4.5°C at specimen mid-height, +5°/-3°C at the base, and 0°/1.8°C aboveground 20 mm below the specimen base. The variations of this last sensor are very small due to the influence of bath temperature, which has been set at 2°C 0.5°C for the test duration. The instrumentation layout thus produces a non-homogeneous vertical thermal gradient within the specimen.

These measurements however only reveal small temperature deviations in any cross-section between temperatures measured at the sample core and at its edge, which serves to validate the testing protocol. For the following study, the temperature indicated at the specimen periphery has been selected as the reference temperature.

• Strain measurements:

Strain gauges (30-mm long, 120 ohms, sold under the KYOWA brand) were installed on a flat section laid out at the specimen periphery, for the dual purpose of providing a flat surface to fasten the gauges while avoiding edge effects related to the compaction mould. The sawed and cleaned specimen surface was impregnated with a primer coat, so as to fill pores on the AC for subsequent bonding improvement. The strain gauge was bonded vertically onto this surface, perpendicular to the direction of freezing propagation; it was then connected to the power supply cables and covered by a special paste and protective ribbon on an aluminium sheet, thereby protecting the gauge from humidity.

Since these strain gauges are sensitive to temperature variations, it becomes necessary to correct the acquired signal. Along these lines, an identical gauge was introduced under the same test conditions; it was bonded onto a silicate bar with near-zero strain, given its very low coefficient of thermal dilatation, i.e. equal to $0.03 \cdot 10^{-6}$ K^{-1} (which is negligible in comparison with the coefficient for road ACs, i.e. on the order of $30 \cdot 10^{-6}$ K^{-1}).

Then taking the difference between the measured strains in the AC and in the silicate bar, it makes it possible to reach the real strain within the AC specimen.

The complete specimen instrumentation layout is indicated in **Figure 12**.

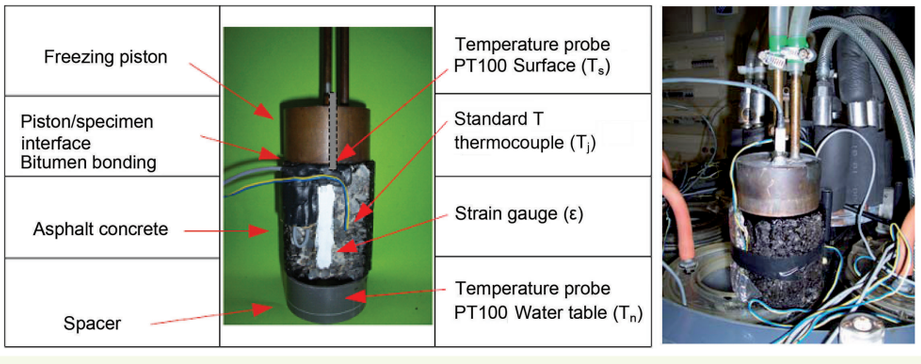

Figure 12
Sample instrumentation and implementation in the freezing cell

For the purpose of validating the test protocol, contraction/expansion measurements were performed on a stainless steel sample with a known thermal coefficient; these results revealed a very high level of agreement between calculated and measured values.

Results of testing on asphalt concretes

› Evolution in axial strain: Determination of the coefficient of dilatation

Thermal strain (dilatation/contraction) in pure mode (i.e. stress-free) of a material is typically expressed via the coefficient of thermal expansion (whether volumetric or linear), denoted α:

$$\alpha = \frac{d\varepsilon^T(T)}{dT} \qquad [1]$$

where ε^T is the strain (volumetric or linear) and T the temperature.

Over a given temperature range $[T_1, T_2]$, the average coefficient of dilatation is defined by:

$$\alpha_m = \frac{\varepsilon^T(T_2) - \varepsilon^T(T_1)}{T_2 - T_1} \qquad [2]$$

Testing conducted on the various samples AC-33, AC-34 and AC-36 began at room temperature (18°C) and continued by decreasing temperature at a rate of 20°C/hour until reaching -10°C at the top of specimens; it was then held at -10°C for 11 hours and raised at the same 20°C/hour rate until a temperature of +10°C was recorded at the specimen surface.

The temperature at specimen mid-height, considered as the average specimen and gauge temperature, is represented in **Figure 13** (upper curve, right-hand scale).

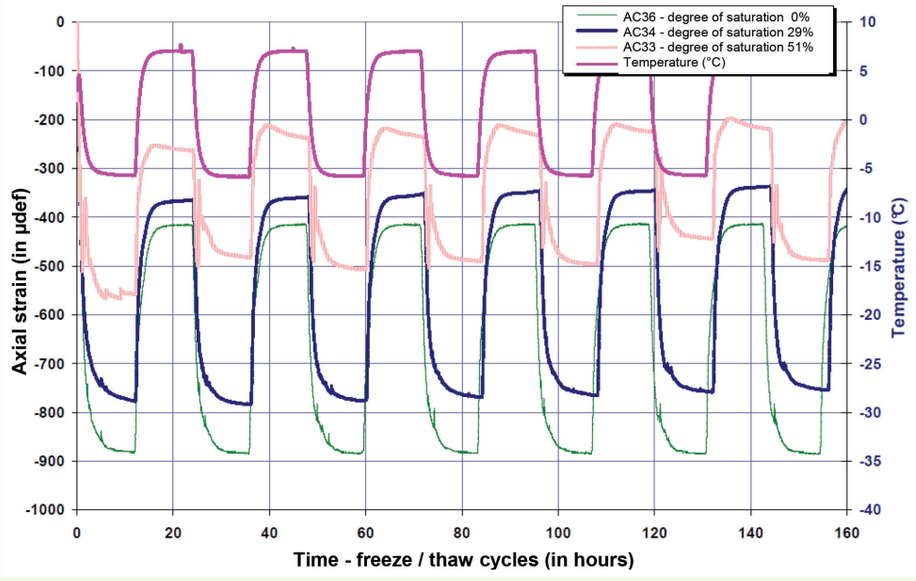

Figure 13
Evolution of both temperature and strain vs. the number of thermal cycles

This figure compares the thermal strains of all three specimens at different degrees of saturation, vs. the number of freeze-thaw cycles. The thermal strain has been arbitrarily set to zero at the initial test temperature +10°C.

For the dry specimen (i.e. AC-36), the variation in ε^T is nearly proportional to the temperature variations recorded during the thermal cycles, whether in cooling or warming. The value obtained for the average coefficient of linear dilatation of sample AC-36, within the temperature variation range (+10°C / -5°C), equals $34 \cdot 10^{-6}$ K^{-1}. This value lies in the interval listed in the bibliography (Di Benedetto and Neifar, 1997), which allows validating the entire measurement and correction protocol (based on use of the silicate bar).

When the test is conducted on the sample with limited water saturation (i.e. AC-34), the coefficient α_m decreases slightly to a value of $30 \cdot 10^{-6}$ K^{-1}. When the degree of saturation reaches 51% (AC-33), the (apparent) coefficient α_m, as measured over this same temperature interval, drops more abruptly to a value of $23 \cdot 10^{-6}$ K^{-1}. At this point, it becomes interesting to examine in greater detail the trend in strains at the scale of a single cycle.

These curves are described in detail in **Figure 14**; they represent the trend in strains recorded on each sample throughout the first seven hours of the first cycle, during which time the temperature is monotone decreasing.

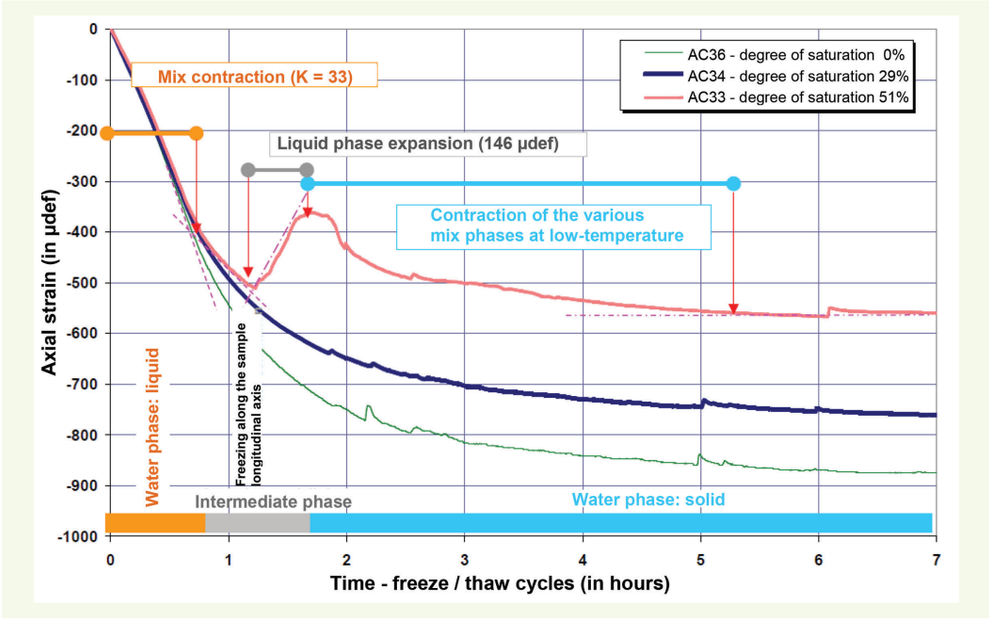

Figure 14
Effect of degree of saturation on sample contraction and dilatation

Let's note the very sharp difference in behaviour between samples AC-33 and AC-36. The dry sample AC-36 undergoes a monotone decreasing strain that is nearly homothetic to the temperature curve, since it reaches during the thermal plateau phase a strain of approx. 880 µdef. Sample AC-33, saturated at 51%, displays a 3-stage evolution. At positive temperatures, its strain is nearly indistinguishable from that of the dry sample. During the subsequent period, as temperature drops below 0°C, its rate of evolution slows (in absolute value terms) until the time it quite suddenly enters a phase of significant swelling (on the order of 150 µdef), as measured based on the concave part of the trend curve. Next, it resumes a contracting evolution that basically remains parallel to the dry sample curve. The two curves wind up being offset by a value on the order of 300 µdef (swelling + difference recorded before swelling), as reflected in the difference observed above on the average coefficients of dilatation. Sample AC-34, saturated at 29%, behaves qualitatively like the dry sample, without exhibiting any expansion when transitioning to 0°C temperature. The presence of water is indicated however by a slower strain rate, leading to a deviation of approx. 100 µdef.

These tests have thus effectively highlighted a characteristic effect of AC swelling when crossing the freezing front, once their water saturation exceeds a given threshold. This effect is to be attributed, like in soils, to the phase change from "liquid water into ice" for water contained in the pores, which is accompanied by constant pressure with a volumetric dilatation of approx. 10%.

In contrast, both before and after crossing the freezing front, the thermo-mechanical behavior of AC-33 is identical to that of a solid whose strains are proportional to the temperature variation. Moreover, the coefficients of dilatation over the course of these phases remain similar to those of the dry AC: for positive temperatures, the partial sample saturation (and free-flow conditions at the boundaries) make it possible to absorb, without inducing any effects, the sizable dilatation

differential between liquid and solid; while at low temperature, as the liquid/ice transition is taking place, the relatively small quantity of ice present inside the solid matrix conceals the dilatation differential between ice and the mineral phase of the AC.

Put in other terms, the behaviour observed on specimen AC-33 can be described schematically by the following equations:

$$\varepsilon^T = \alpha(\theta - \theta_i) \text{ si } \theta > 0 \quad [3]$$

$$\varepsilon^T = \alpha(\theta - \theta_i) + \varepsilon_{swelling}(S_r) \text{ si } \varepsilon^T = \alpha(\theta - \theta_i), \quad [4]$$

in assuming, for the sake of simplification, both that swelling $\varepsilon_{swelling}$ suddenly occurs at 0°C temperature and that the coefficients of dilatation for the AC at strictly positive and negative temperatures are equal. The strain $\varepsilon_{swelling}$ depends on the degree of AC saturation: it equals zero for and increases with saturation rate.

The more gradual evolution of actual strain measurements on sample AC-33 undoubtedly indicates more gradual swelling than what has been assumed herein, yet undeniably also stems in part from the finite (and extensive) length of the gauges, which have been laid out perpendicular to the freezing front propagation direction (see insert).

GAUGE SIGNAL MODELLING WITHIN THE FRAMEWORK OF EQUATIONS [3] AND [4]

Let's begin by denoting l the gauge length and $z_f(t)$ the freezing front position, which is assumed to exhibit a vertical extension and coincide with the condition $\theta(z,t) = 0$. According to Equations [3] and [4], by considering the times at which the freezing front is located between the bottom and top of the gauge:

$$\varepsilon^T{}_{gauge}(t) = \frac{1}{l}\left(\int_{zbottom}^{zf(t)} \alpha(\theta(z,t) - \theta_i)dz + \int_{zf(t)}^{ztop} (\alpha(\theta(z,t) - \theta_i) + \varepsilon_{swelling}(S_r))dz\right)$$

$$= \frac{1}{l}\int_{zbottom}^{ztop} \alpha(\theta(z,t) - \theta_i)dz + \varepsilon_{swelling}(S_r)\frac{z_{top} - z_f(t)}{l}$$

In terms of strain rate, the following can be deduced:

$$\frac{d\varepsilon^T{}_{gauge}(t)}{dt} = \frac{\alpha}{l}\int_{zbottom}^{ztop} \frac{\partial\theta}{\partial t}(z,t)dz + \varepsilon_{swelling}(S_r)\frac{v_f}{l} = \alpha\frac{d\bar{\theta}}{dt} + \varepsilon_{swelling}(S_r)\frac{v_f}{l}$$

with $\bar{\theta}$ = average temperature over the gauge length,

v_f = velocity of the freezing front (counted positively when heading downward).

When the freezing front lies above or below the gauge: $\frac{d\varepsilon^T{}_{gauge}(t)}{dt} = \alpha\frac{d\bar{\theta}}{dt}$.

Accordingly, during the time when the gauge is crossed by the freezing front, strain results from both the terms $\alpha\frac{d\bar{\theta}}{dt}$, which is negative during the cooling phase, and $\varepsilon_{swelling}(S_r)\frac{v_f}{l}$, which moves positively as the front lowers.

At any given point in time, this last term can therefore reverse the measurement variation direction, provided the material saturation rate and associated swelling deformation are high enough (which is the case with specimen AC-33).

The evolution exhibited by specimen AC-34 would correspond to the intermediate case of a saturation rate and associated swelling deformation too small to reverse the trend in measured strain rate, yet still sufficient to significantly slow evolution.

More accurate simulations, through use for example of the GEL1D software by ALIZE or the GEL module of the CESAR-LCPC code, would serve to fine-tune the model/measurement comparison and better quantify the values of all pertinent parameters.

Conclusions drawn from the tests on asphalt concretes

These initial results of freeze-thaw tests are instructive as regards the unique behaviour of ACs with high levels of water saturation. Above all, they expose sudden and substantial swelling that arises in the vicinity of the freezing front, i.e. on the order of 150 to 300 µdef (depending on the given mode of determination) for a 51% saturated specimen.

It is plausible that such phenomena can arise *in situ*, under stressful conditions, by means of abrupt pavement degradation. The restricted swelling within layers required to remain flat is basically of a type to generate internal shear stresses, or even tensile stresses, capable of causing debonding between layers or a loss of material cohesion and then forming potholes. The differentiated thermo-mechanical behaviour of materials with distinct properties or displaying different degrees of water saturation can, if applicable, accentuate this phenomena.

Future freeze-thaw laboratory testing of dual-layer AC structures has been planned specifically to investigate this aspect. It will also be worthwhile to characterize the viscoelastic behaviour of ACs with high water content subjected to the freezing effect, so as to identify an eventual loss of their stress relaxation capacity, which would contribute under typical conditions to moderating the development of internal stresses. Moreover, a "testing the water" protocol will allow assessing the risks of raising AC saturation levels by means of the cryo-suction effect in the presence of nearby water "sources" (e.g. infiltration in the event of freeze-thaw phase alternation with precipitation).

CONCLUSION AND OUTLOOK

In order to answer road network managers' questions regarding sustainable repairs to be implemented and the risks of new degradations appearing in heretofore intact zones, it is necessary to understand the mechanism(s) behind such degradations. The circumstances affecting the appearance of these disorders lead to distinguishing a standard and quick-acting mechanism that strips plates of material at the pavement surface from longer-term damage mechanisms capable of acting at more typical, or even higher, temperatures and preparing the "ground" for pothole formation. The quick-acting mechanism would be taken into consideration in the instructive case of boundary situations, subsequent to deficient combinations involving road material choice and both maintenance and operations strategies.

In the search for long-term mechanisms, the instrumentation installed in the surface layers of a structure tested on the LCPC (IFSTTAR) pavement fatigue carrousel has revealed (through application of high temperature) the presence of significant sliding between layers, even ones that are perfectly bonded (Vulcano-Greullet *et al.*, 2010). This finding may, in conjunction with other causes (e.g. stripping in the presence of water), yield an interface damage mechanism that, if confirmed by other measurements, could lead to recommending limiting the number of interfaces as part of a maintenance strategy as well as specifying minimum layer thickness values.

A mechanism able to explain the sudden nature of these disorders, strictly correlated with freeze-thaw transitions, has been updated for ACs partially saturated in water. Free of mechanical stresses, these ACs are prone to major and sudden swelling effects when crossing a freezing front. The tests conducted as part of the Fondephy project have enabled measuring considerable swelling, i.e. on the order of 150 µdef (or even 300 µdef as a differential with a dry AC) for an approx. 50% saturated specimen at the time of freezing. The case of a multilayer pavement structure, where such a mechanism would be constrained, may cause internal stresses capable of loosening material cohesion in the vicinity of layer interfaces (Mauduit *et al.*, 2010). This hypothesis deserves further examination by other measurements and laboratory testing, which is to be practiced not only on homogeneous materials but also on multilayer structures, for the purpose of determining the actual impact of this phenomenon from among all other parameters involved in these disorders.

The set of French standards and technical guidelines must address road network aging in addition to their accompanying pathologies and challenges. The disorders appearing over these past few winters have shown that the method applied for many years in France is indeed subject to criticism. Once the phenomena have been identified and understood, it will perhaps be suitable to incorporate new design tests for AC, ensuring their resilience to freeze-thaw cycles and ensure that design, dimensioning and maintenance methods pay closer attention to interface operations at the various temperature points as well as to the risks of water accumulation inside the pavements. Towards this end, it would be beneficial to develop a high-efficiency, non-destructive diagnostic method that enables quickly detecting vulnerable zones prior to maintenance work (Castaneda Pinzon, 2004; Castaneda and Such, 2004). It would also perhaps be a good idea to intensify reliance on the "radar" or "Colibri" investigation techniques (Simonin and Lièvre, 2006), not just for the purpose of verifying layer bonding or thickness, but also for detecting the presence of trapped water.

ACKNOWLEDGMENTS

The authors would like to thank Jean-Luc Delorme for his valuable support during the research program presented in this article.

REFERENCES

Boutonnet M., Livet J. (1990). Rapport interne sur l'effet du salage sur les températures de surface, Laboratoire Régional des Ponts et Chaussées de Nancy.

Castaneda Pinzon E.A. (2004). *Contribution de méthodes non destructives à l'évaluation de l'effet de l'eau sur les enrobés bitumeux*, Thèse de Doctorat de l'Université de Nantes.

Castaneda E., Such C. (2004). Evaluation of moisture sensitivity of bituminous mixtures by a complex modulus approach, *Transportation Research Record: Journal of the Transportation Research Board*, 1891, TRB, National Research Council, Washington D.C., pp. 62-67.

Delorme J.L. et al. (2007). *Manuel LPC d'aide à la formulation des enrobés à chaud*, Études et Recherches des Laboratoires des Ponts et Chaussées, LCPC.

Di Benedetto H., Neifar M. (1997). Coefficients de dilatation et de contraction thermiques d'un enrobé bitumineux avec et sans chargement mécanique, *Mechanical Tests for Bituminous Materials, Di Benedetto & Francken Editors*.

Fromm H.J., Phang W.A., Noga M. (1965). *The incidence of stripping and cracking of bituminous pavements in Ontario*. Proceedings of Canadian technical asphalt association, Vol. 10, pp. 157-179

Hammoum F., Hornych P. (2004). Quantitative study of bituminous materials microstructure by digital image analysis. *Proceedings, 3rd Eurobitume & Euroasphalt congress*, Vienne (Autriche).

Hicks R.G. (1991). *Moisture damage in asphalt concrete.* National cooperative highway research program: synthesis of highway practice, Report 175.

Kandhal P.S; Lubold C.W., Roberts F.L. (1989). Water damage to asphalt overlays: cases histories.*Meeting of the Association of Asphalt Paving Technologists*, National Center for Asphalt Technology Nashville (Tennessee).

Kandhal P., Rickards I. (2001). Premature failure of asphalt overlays from stripping: cases histories. *Proceedings of the Association of Asphalt Paving Technologists*, Clearwater (Floride). Volume 70, pp. 301-343.

Mauduit C., Hammoum F., Piau J.M., Mauduit V., Ludwig S., Hamon D. (2010). Quantifying dilation effects induced by freeze–thaw cycles in partially water saturated bituminous mix: Laboratory experiments. *Road Materials and Pavement Design, EATA special issue*, Parme Italie.

Mauduit C., Mauduit V. (2006). Rapport d'étape n°1, *Opération Fondephy du LCPC*.

Mauduit V., Mauduit C., Vulcano-Greullet N., Coulon N. (2007). Dégradations précoces de couches de roulement à la sortie des hivers, *Revue Générale des Routes et Aérodromes, N° 858*, pp 67-72.

Sétra-LCPC (1997). *French design manual for pavement structures*. Laboratoire Central des Ponts et Chaussées and Service d'Études Techniques des Routes et Autoroutes.

Simonin J.M., Lièvre D. (2006). Compte rendu des essais Colibri – mesures sur la RN4 près de Ménil-la-Horgne (Meuse) du 21 au 23 mars 2006, LCPC.

Vulcano-Greullet N, Kerzreho J.P., Chabot A., Mauduit V. (2010). Stripping phenomenon of top layers of thick pavements. *Congrès ISAP2010*, Nagoya, Japan.